Hydrobiologia (2008) 612:269–279
DOI 10.1007/s10750-008-9496-8

FISH HABITAT MAPPING

Satellite observations of main oceanographic processes to identify ecological associations in the Northern Arabian Sea for fishery resources exploration

Himmatsinh U. Solanki · Pradip C. Mankodi · Rashmin M. Dwivedi · Shailesh R. Nayak

Abstract Ecological associations are the inter-relationship between the species and their environment. Oceanographic processes like upwelling events and formation of eddies, rings, and fronts have been monitored using National Oceanic and Atmospheric Administration Advanced Very High Resolution (NOAA AVHRR) and Indian Remote Sensing Satellite-P4-Ocean Colour Monitor (IRS-OCM) data. Sea Surface Temperature (SST) and chlorophyll concentration (CC) images were derived from AVHRR and OCM, respectively. Upwelling event was monitored using AVHRR-SST by detecting the differences in surface water temperature. The formation of eddies, rings, cyclonic eddies, and anti-cyclonic eddies and their biological responses were studied using CC. Eddies and rings were found with high phytoplankton production in the form of bloom, which provide grazing ground for fishes. The anti-cyclonic eddies were found with very low CC, indicating the biological deserts in the ocean. The impacts of these processes on fish catch were studied using fishing operations data procured from Fishery Survey of India. In this paper, the occurrence of different oceanographic processes, their persistence, and relevance with catch statistics of fishery resources in the study area are discussed. The study explains the potentials of satellite remote sensing to establish the habitat linkage between oceanographic processes and fishery resources.

Keywords Oceanographic processes · Satellite · Remote sensing · Fisheries

Guest editor: V. D. Valavanis
Essential Fish Habitat Mapping in the Mediterranean

H. U. Solanki (✉) · R. M. Dwivedi · S. R. Nayak
Marine Water Resources Group, Space Applications Centre (ISRO), Ahmedabad 380015, India
e-mail: himmatsinh@sac.isro.gov.in

P. C. Mankodi
Faculty of Science, Maharaja Sayajirao University of Baroda, Fatehgunj, Vadodara, Gujarat 390002, India

Introduction

Marine earth observations (EO) from satellites are particularly suitable for sampling and monitoring large areas. The major EO products about the ocean's surface include temperature distribution and chlorophyll concentration. Several Remote Sensing techniques can provide information regarding surface circulation features that affect or define fish habitats. These include the location and evolution of frontal boundaries, upwelling areas, currents, and circulation patterns in general. Optical and thermal characteristics of surface waters can be used as natural tracers of dynamic patterns. Understanding the physical and biological processes, as well as their interactions, is a central goal for fisheries management over continental shelf areas. A complex suite of seasonal physical processes influences phytoplankton productivity and fisheries production.

Satellite remote sensing applications in fisheries have concentrated on the measurements of ocean temperature, ocean color, and computation of ocean water transport based on satellite-measured wind stress (Laurs & Burcks, 1985). Examples of potential use of satellite imagery in the eastern North Pacific fisheries were given by Fiedler et al. (1985). Yamanaka et al. (1998) described the utilization of satellite imagery in Japanese fisheries. Njoku et al. (1986) reviewed applications of thermal infrared imagery in oceanography. Satellite imageries and concurrent albacore catch examined by Laurs et al. (1984) demonstrated that the distribution and availability of albacore are related to oceanic fronts. They substantiate the conventional wisdom of many fishermen who use temperature and/or color "breaks" to locate potentially productive fishing areas for albacore. Authors speculated that the behavior mechanisms related to feeding might be responsible for tuna aggregation on the warm side of temperature front. To support this argument the authors use Coastal Zone Colour Scanner (CZCS) measurements along with knowledge that tuna are visual feeder. Maul et al. (1984) combined in situ observation from four research vessels, CPUE (catch-per-unit-effort) for Atlantic blue fin tuna, visible (CZCS) and thermal infrared (GOES, NOAA) satellite data of Gulf of Mexico. The boundaries gulf loop current was located using satellite data during 1980 in fishing areas. CPUE was analyzed and a threefold increase in tuna catch in 1980 over that in 1979 was observed using available satellite infrared and visible imagery. Sugimoto & Tameish (1992) observed that warm and cold streamers entrained the periphery of the warm core ring, which form excellent fishing ground for pelagic fish such as skipjack, mackerel, flying squid, and saury. Stretta (1991) used a variety of satellite data as input in a proposed model for tuna fishing in the Gulf of Guinea region. Podestra et al. (1993) found that the probability of very high catch rates in US longline fishery for swordfish in the Atlantic was greater in the vicinity of SST fronts. Solanki et al. (1998a, b, c) used AVHRR sea surface temperature (SST) data to delineate thermal feature to locate potential fishing grounds and to study seasonal variability in fishery resources based on the patterns of ocean features observed in thermal imagery in the Arabian Sea.

Solanki et al. (2001a) synergistically analyzed SeaWiFS and AVHRR data. They found that ocean color features coincided with thermal boundaries at some locations. This indicates that physical and biological processes are closely coupled at these locations. High fish catch points were found in the vicinity of coincided boundaries. An approach for integration of chlorophyll concentration and SST features has been developed by Solanki et al. (2000) using OCM chlorophyll concentration and AVHRR SST. Some preliminary results of synergistic application of chlorophyll and SST have been demonstrated by Solanki et al. (2001b) for exploring the pelagic resources in the water of Gujarat coast. Gill nets were used for fishing in suggested Potential Fishing Zones (PFZs). Pomfret catch was found to increase twofold. OCM chlorophyll concentration images and AVHRR SST images were used by Solanki et al. (2003a, b) for fishery forecast. Comparatively high CPUE was observed in the PFZs forecast areas as compared to other areas in the Northern Arabian Sea.

Materials and methods

Study area

Figure 1 shows the location of the study area, which is a high productive region, off the Gujarat Coast in the Northern Arabian Sea that supports extensive fishing grounds. Gujarat State has the longest coastline of 1,640 km among the maritime States of India. The continental shelf area along the State (Latitude 20–23° N) is about 90,200 km^2, the largest shelf area among the Indian maritime States with a maximum continental shelf width of about 191 miles. The gradient of the shelf area is 1:1,769 at the maximum width and 1:537 at the minimum width. The powerful cyclonic Somalia current grazes the Saurashtra coast during the southwest monsoon. During the northeast monsoon, off-shore winds along the Kathiawar peninsula induce the primary production and high fish production.

OCM data for chlorophyll concentration and AVHRR data for SST computation were used. PFZs fish catch data, collected by the survey vessels (*Matsya Nireekshani* and *Matsya Mohini*) of Fishery

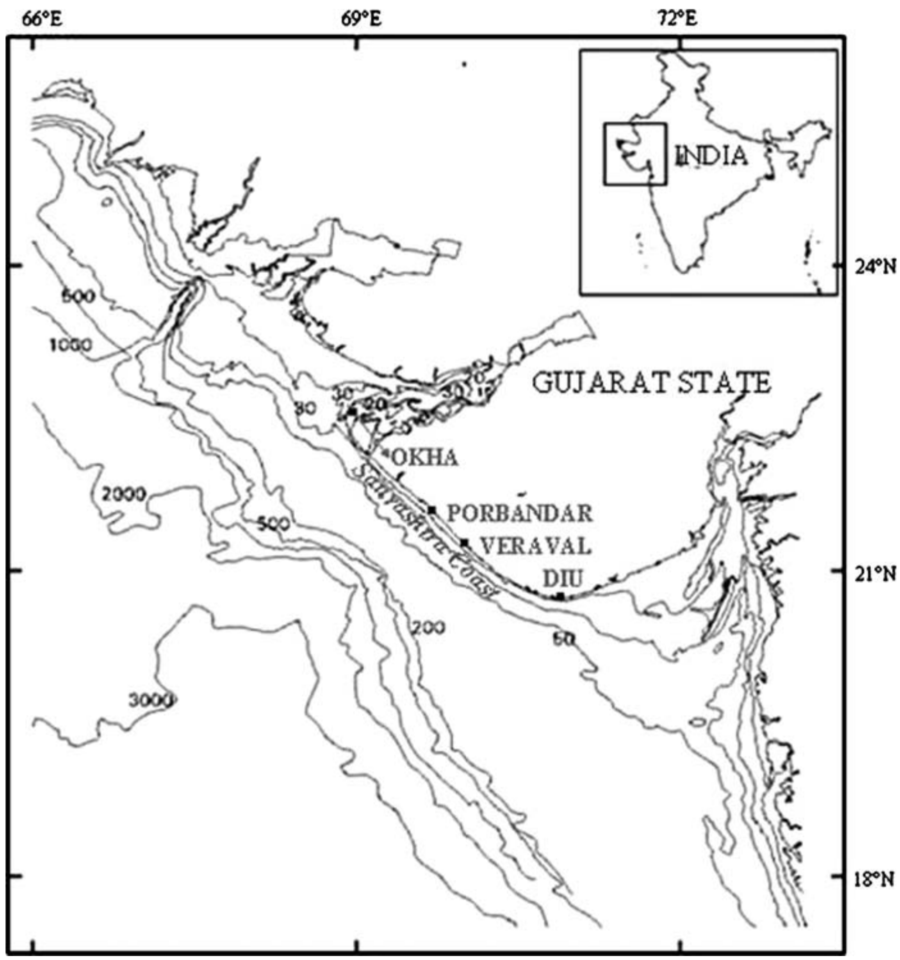

Fig. 1 A map showing the study area off Gujarat coast, north west coast of India, Northern Arabian Sea. Depth contours are in meters

Survey of India (FSI), were used in the study (Anonymous, 1996). The major species caught were ribbon fish, catfish, horse mackerel, sciaenids, decapterids and nemipterids, and squids. Fish catch data were normalized and classified in terms of CPUE. The fish catch classification was based on mean (μ) and standard deviation (SD). Mean (μ) of catch is considered as normal catch in the area. The details of statistical analysis, fishing gear, and species caught during fishing operation are discussed by Solanki et al. (2005). The catch points were classified with a combination of mean and standard deviation. Gujarat State fisheries data was available for daily trips. They were normalized as kg/hr with consideration of fishing hours. The catch composition consists of horse mackerels, lesser sardines, ribbon fishes, squids, and *Sciaenis*.

Satellite sensor data analysis

OCM data analysis

The retrieval of ocean color parameters such as phytoplankton pigment (i.e., chlorophyll concentration) and suspended matter in near shore waters involves two major steps. The first is known as atmospheric correction of visible channels to obtain normalized water leaving radiance and the second is the application of bio-optical algorithms for water parameters retrieval. The process of retrieving water leaving radiance L_w from the total radiance measured at the sensor L_t is usually referred as atmospheric correction. The ocean color parameters such as chlorophyll concentration and suspended matter concentration are estimated from the retrieved spectral water leaving radiance by the application of suitable bio-optical algorithms.

Atmospheric correction of IRS-P4 OCM imagery

In oceanic remote sensing, the total signal received at the satellite altitude is dominated by radiance contribution through atmospheric scattering processes and only 8–10% of the signal corresponds to oceanic reflectance. Therefore, it becomes mandatory to correct for atmospheric effect, to retrieve any quantitative parameter from space. A long wavelength approach suggested by Gordon et al. (1985) and Mohan et al. (1998) was adopted for atmospheric correction of optical data. It has been shown that for near infrared (NIR) channels, the water leaving radiance coming out of ocean can be approximately considered equal to zero (Gordon et al., 1985). The radiance received by a satellite sensor at top of the atmosphere (TOA) in a spectral band located at a wavelength λ_i, $L_t(\lambda_i)$ can be divided into following components:

$$L_t(\lambda_i) = L_a(\lambda_i) + L_r(\lambda_i) + T(\lambda) * L_g(\lambda_i) + t(\lambda_i) * L_w(\lambda_i)$$

where L_a and L_r are radiance generated along the optical path by scattering in the atmosphere due to aerosol and Rayleigh scattering, L_g is the specular reflection or sun glint component, and L_w is the water leaving radiance.

TOA radiance in OCM channels 765 and 865 nm mainly correspond to the contribution coming only from atmosphere, since water leaving radiance L_w (765 & 865 nm) can be safely assumed to be equal to zero. The Rayleigh scattering term (L_r) is computed using well-established theory. Once L_r is known then L_t is assumed equal to L_a, i.e., the aerosol path radiance. OCM payload has two channels at 765 and 865 nm in NIR and a relationship is obtained for the spectral behavior of the aerosol optical depth from these two bands. An exponential relationship for spectral behavior of aerosol optical depth has been used for atmospheric correction algorithm. The aerosol optical thickness has been extrapolated to visible channels using this exponential relation. Rayleigh scattering and sun glitter components were also computed based on the method by Mohan et al. (1998).

Bio-optical algorithms for OCM imagery

A number of bio-optical algorithms for chlorophyll retrieval have been developed to relate measurements of ocean radiance to the in situ concentrations of phytoplankton pigments. An empirical algorithm (also known as Ocean Chlorophyll 2 or OC2, O'Reilly et al., 1998) has been used with IRS-P4 OCM data, on the basis of results of a study on inter-comparison of different bio-optical algorithms. This algorithm was modified as per regional retrieval of chlorophyll concentration (Chauhan et al., 2002). It has been found that this algorithm captures the inherent sigmoid relationship between $R_{rs}490/R_{rs}555$ band ratio and Chlorophyll concentration C (where R_{rs} is remote sensing reflectance). The algorithm was shown to retrieve low as well as high chlorophyll concentration which means a better retrieval. The algorithm operates with five coefficients and has following mathematical form:

$$\log_{10} C = 0.341 - 3.001 * R + 2.811 * R^2 - 2.04 * R^3 \text{ for } 0.01 \text{ mg/m}^3 \le C \le 50 \text{ mg/m}^3$$

where C is chlorophyll concentration in mg/m^3 and $R = \log_{10}[R_{rs}(490)/R_{rs}(555)]$, where R_{rs} is remote sensing reflectance.

The chlorophyll concentration images were generated using the aforementioned processing approach. The software for generating chlorophyll concentration images is available for operational use at laboratory of Marine and Water Resources Group, Space Applications Centre, Ahmedabad.

AVHRR data analysis

The brightness temperature sensed at satellite height is influenced mainly by atmospheric moisture. The signal loss due to water vapor absorption is proportional to the radiance difference in the measurement made at two different channels of the thermal infrared. The multi-channel sea surface temperature (MCSST) approach suggested by McClain et al. (1985) was used to compute SST from AVHRR thermal infrared channels, i.e., Channel 4 (10.3–11.3 µm) and Channel 5 (11.5–12.5 µm). In order to estimate SST accurately, it is necessary to eliminate the influence of emission from clouds besides the precise calibration and navigation. Prior to the SST estimation, pixels of full-resolution images are discriminated into cloud-free pixels or cloud-contaminated pixels using a cloud-filtering algorithm, i.e., threshold tests for reflectance, brightness temperature and brightness temperature difference between the split-window channels. SST is estimated from the brightness temperature of cloud-free pixels of the split-window channels using the following linear regression equation of the Multi-channel SST (MCSST) retrieval algorithm (McClain et al., 1985)

$$SST = a \cdot T_{11} + b(T_{11} - T_{12}) + c(T_{11} - T_{12}) \cdot (\sec\ \theta - 1) + d$$

where T_{11} is brightness temperature in 11 μm band, T_{12} is brightness temperature in 12 μm band, θ is satellite zenith angle, and a, b, c, and d are coefficients of the linear regression equation. The coefficients of the equation for each satellite and for daytime or nighttime are provided on the web site of National Environmental Satellite Data and Information Service (NESDIS) of NOAA. After the estimation of SST, the estimated value in each pixel is compared with the climatology values of SST in order to eliminate unreasonable values of SST.

Preliminary geometric correction was carried out according to Narayana et al. (1995). This approach uses the satellite ephemeris. The precise geometric corrections were carried out using a set of ground control points (GCPs) located both on an image and on a Naval Hydrographic Office (NHO) bathymetric map. This geo-reference master image was used to image registration of AVHRR channels in order to generate geo-reference data set. Color-coded SST images were generated which indicate the distribution of SST in the northwest Arabian Sea. Same color scheme was applied to both chlorophyll and SST images to facilitate comparison between two parameters.

Results and discussion

Satellite observation of coastal upwelling formation processes

Satellites are very useful to locate and monitor coastal upwelling, which required frequent observation over the large area. Time series AVHRR SST imagery for September and October 1995 were analyzed to study various phases of the upwelling process in the Arabian Sea. Figure 2 indicates monitoring of different upwelling phases occurred during the event. The coastal upwelling offshore Gujarat coast was initiated in September 1995. It is clearly observed in the images of SST derived from NOAA AVHRR data (September 28, 1995). This image indicates the maturation phase of upwelling extending from Okha to Diu. During this phase, the phytoplankton growth starts as nutrient supply in the euphotic zone, which enhances the primary production in the upwelling area. This phase creates favored fish feeding grounds as simultaneous zooplankton and herbivorous fish accumulate in the upwelling zone.

Figure 3 indicates weekly mean fish catch during the period of persistent upwelling. The fishing season usually starts after monsoon in September along the Gujarat Coast. Pre-upwelling weeks indicate that normal catch and fish catch decline during the initiation phase. As primary production increases due to availability of nutrient rich water during the maturation phase, an increase in fish catch during this phase and continued in stabilization phase is observed (Solanki et al., 1998a).

Satellite observations of cyclonic eddies and rings formation processes

The cold core eddies and rings can initially be characterized by low temperature and salinity, high nutrient concentration and great biological activity. Satellite observations are limited to SST and biological production (chlorophyll concentration). Rings transport both nutrients and biota. The transported nutrients are important in enhancing oligotrophic conditions. Eddy and ring formation was studied using time series OCM data. The area selected for this study was 20–23° N and 65–68° E. This area is known for eddy formation and high production during winter months (Banse, 1968). Eddies and rings were monitored for several months to study their formation and maturation. The general structure of eddies and rings and their evolution in time are shown in the Fig. 4. This figure indicates eddies and rings formation and decay stages. Four different eddies have been marked with serial numbers. The eddy marked "1" in Fig. 4 formed, developed, and decayed after 1 month. The eddy started forming on March 01, 2004, rotating in anticlockwise fashion and moving toward southwest

Fig. 2 Upwelling event observation in SST image derived from NOAA-AVHRR along the Gujarat coast during October 1995. Different shades of gray along the coast show coastal upwelling process

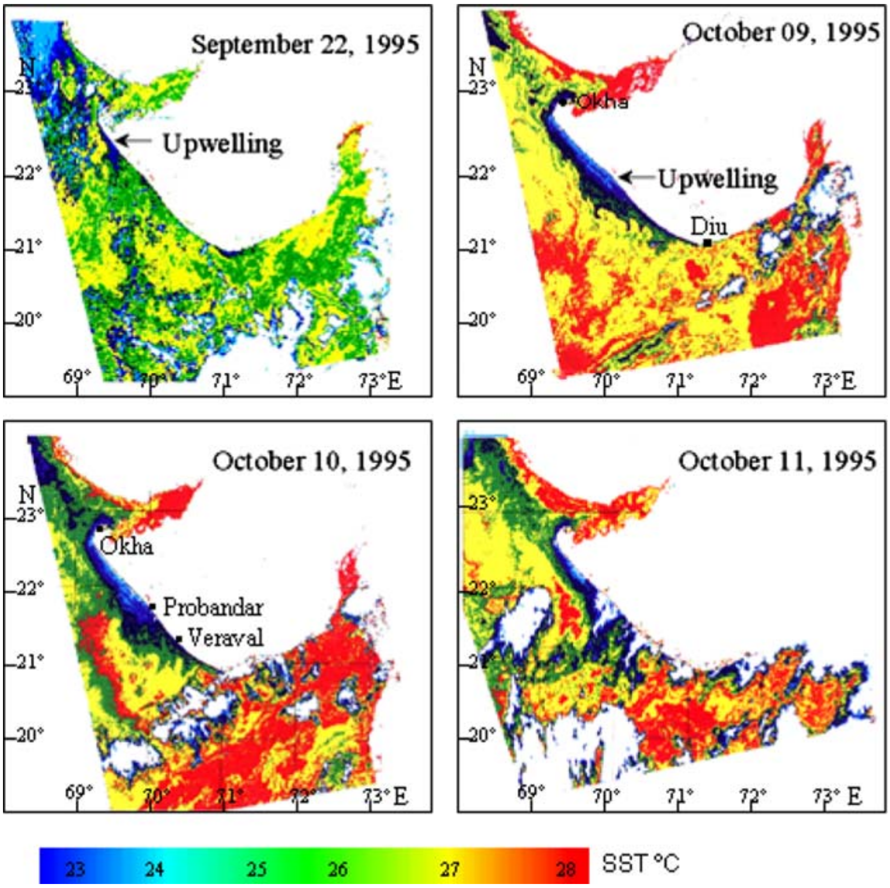

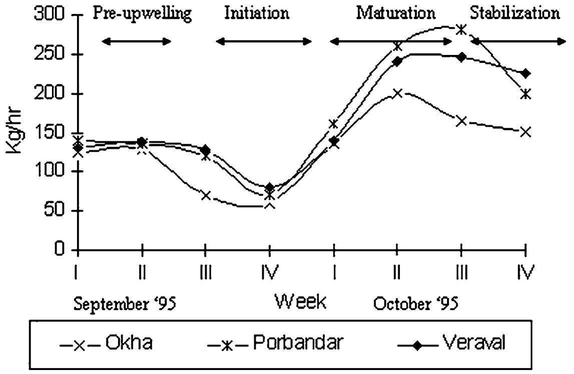

Fig. 3 Fish catch during different stages of upwelling along Gujarat Coast, India

direction, and formed an attached ring during March 21–25, 2004. The ring decayed on March 27, 2004. The feature marked "2" is a ring formed during March 3–5, 2004, in 21–22° N and 67–68° E remaining at the same area for about a month and decayed on March 27, 2004. This ring was highly energetic and supported high production as nutrient supply was continuously available due to rotation of the feature. The feature marked "3" indicates a different stage of eddy formation. This is a weak eddy. It started forming on March 07, 2004, and was found decayed during March 25–27, 2004. The eddy feature marked "4" was observed for only a week. It formed on March 07, 2004 and decayed on March 15, 2004.

With time, mixing and heating modify the surface water properties related to quality and biological production. There are five physical mechanisms leading to the decay of eddies and rings: They are dispersion, instability, interaction with mean flow, small-scale friction, and surface wind mixing and heat exchanges. The sharp biological contrasts that exist at ring formation also decline with time. Chlorophyll concentration is a measure of the phytoplankton biomass and was found highest in the rings. Highest biomass occurs near the center of a ring and progressively declines toward the ring's edge (Fig. 4).

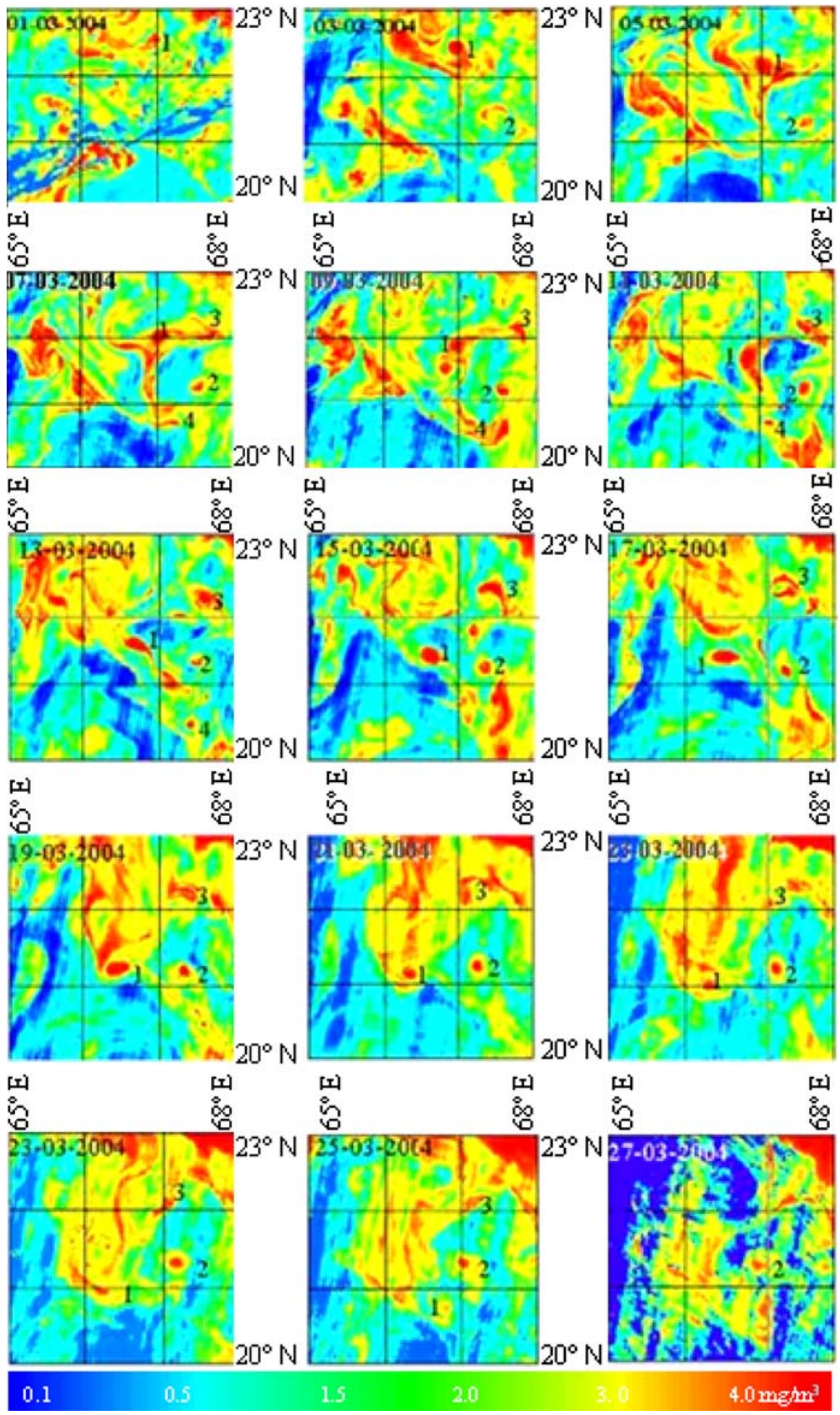

Fig. 4 Observations of cyclonic eddies and rings formation using OCM data

The potential of satellite observation allows its monitoring the formation, persistence of eddies, and their impacts on biological production. The observations are shown on the images of eddies (Fig. 5). High CPUE points were found in the vicinity of eddies and comparatively poor catch points were found in non-

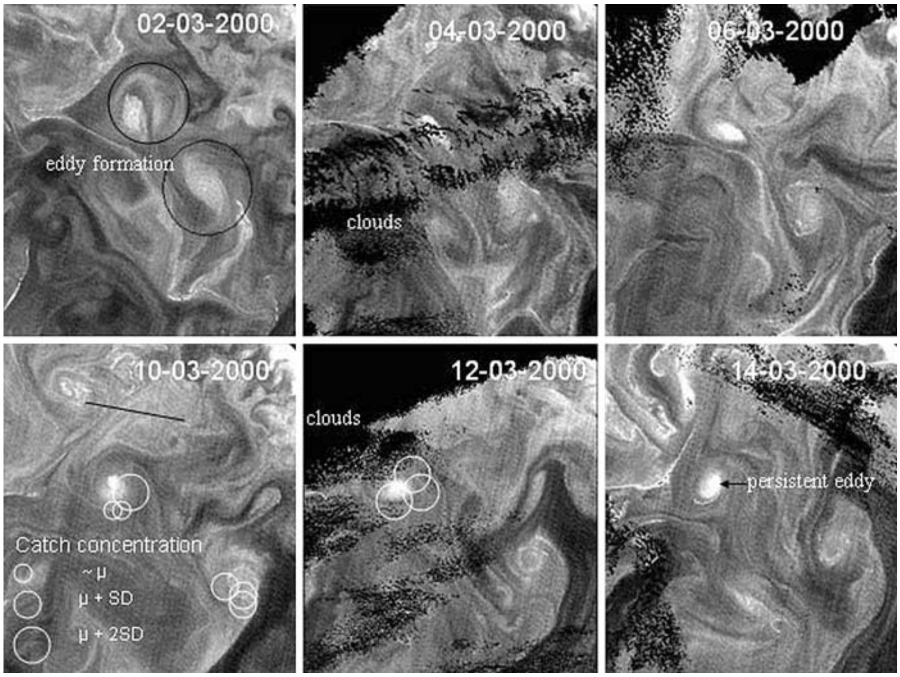

Fig. 5 Sequential images of OCM-derived chlorophyll concentration show eddy formation, their persistence, and their relevance to fish catch. White circles indicate classified fish-based mean (μ) and standard deviation (SD). Darker to lighter tone indicates the lower to higher chlorophyll concentration

eddy areas. Eddies are a moving feature, and hence there is always transport and mixing of nutrients in these areas, which enhances the productivity.

Significance of cyclonic eddies and rings in Northern Arabian Sea

Cyclonic eddies transport nutrient-rich water to sea surface, and an important requirement is fulfilled for an abundant development of plankton in eddy regions. This serves as food for higher organisms, which in turn form the basis of nourishment for edible fish. In this study, a satellite observation of eddies and rings has provided an initial understanding of their behavior. With these data we can assess the influence of rings on the oceanic distribution of physical, chemical, and biological properties. In the ring formation process, a large volume of water is transported across the area. As the ring moves and decays, there is a partial exchange of this water with the surrounding one; thus the rings generate a flux of properties from shelf to open ocean and transfer organic material enhancing biological production.

Satellite observation of anti-cyclonic eddies

Clockwise rotation of eddies accumulate warm water in the center of the eddy. Anti-cyclonic eddies are considered as biological deserts as nutrient-poor warm water with low biological production is accumulated in the center of the eddy (Fig. 6). The area covered by the warm core eddy spread over around 100 km × 100 km area. The formation process was initiated in the third week of February 2003 and lasted for more than 2 weeks.

Monitoring of such ocean event using satellite is very useful for guiding fishermen to avoid operating in such areas. Although, fisheries data were not available for this study area, the structure of such water bodies is important for the life conditions in the ocean. Sun light and nutrients are the essential requirements for the development of phytoplankton growth which is the basis of food for zooplankton, which in turn feeds the higher organisms. An abundant plankton population consumes nutrients and descends dead into deeper layers. Because of the chemical decay processes, the decomposition constituents are again dissolved in the water and contribute

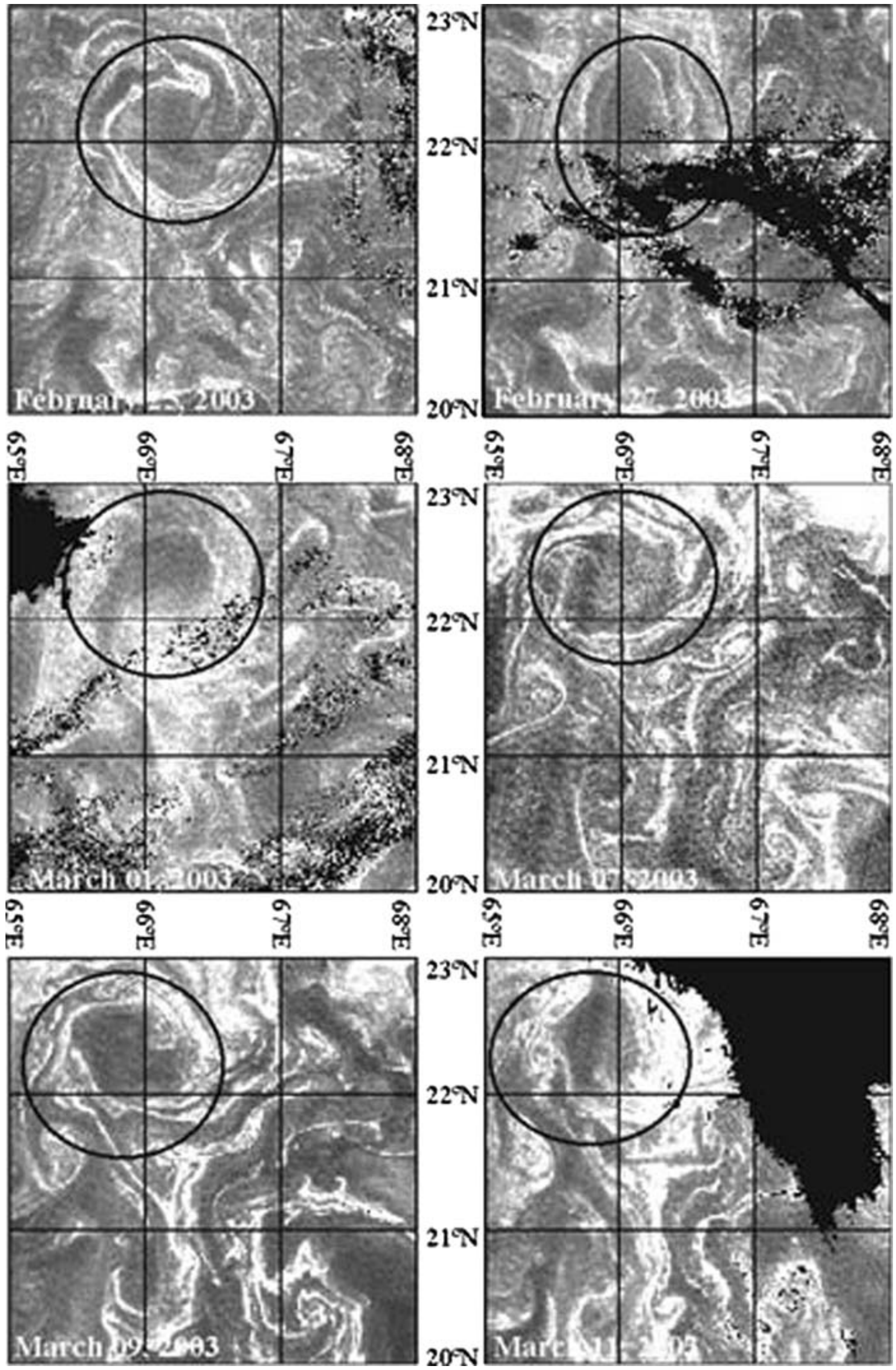

Fig. 6 Satellite observations of anti-cyclonic eddy using OCM data during February–March 2003. Darker to lighter tone indicates the lower to higher chlorophyll concentration. Anti-cyclonic eddy with poor chlorophyll concentration is shown in the circle

to accumulation of nutrients. Therefore, surface water layers near surface lose their nutrients if they are not replenished from deeper layers (upwelling). This is the case with anti-cyclonic eddies that are areas poor in nutrients and do not permit a significant development and growth of micro-organisms.

Satellite observation of fronts

Fronts are important in the ocean dynamics since they are the regions where vertical advection and exchange of momentum are intense. The design of fishing strategies for maximum yields involves the

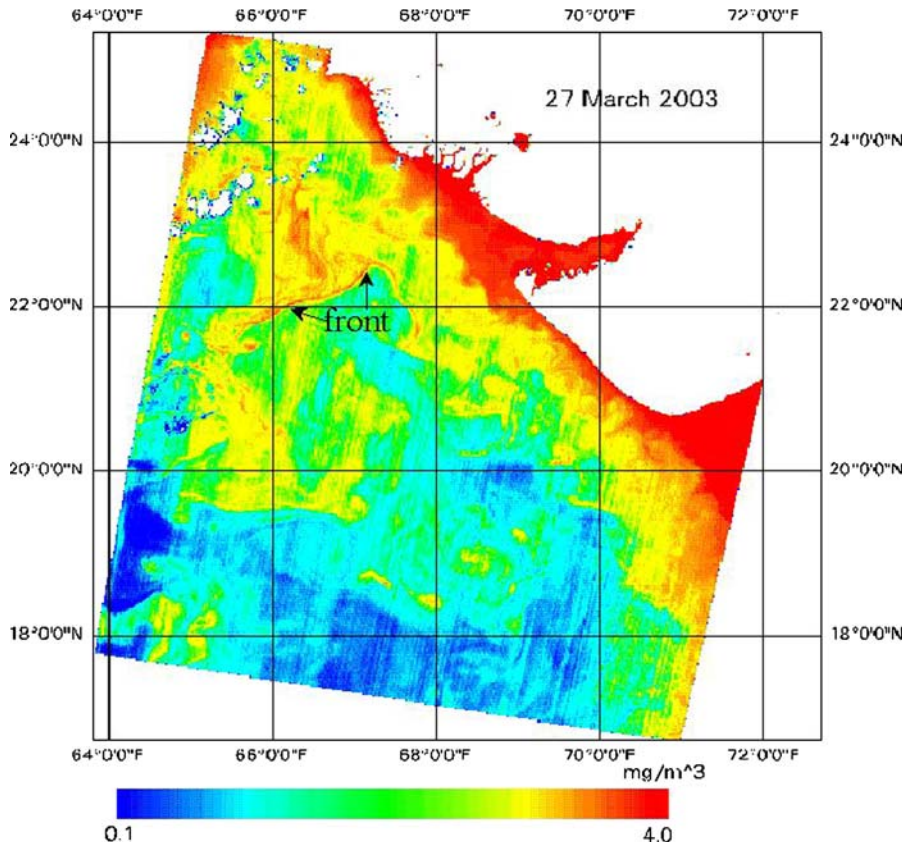

Fig. 7 A typical chlorophyll concentration image shows ocean color front with sharp gradient of chlorophyll concentration and its extent of distribution

detailed knowledge of the location of oceanic fronts where established algal blooms create regions of high biological productivity.

In oceanic front areas, there is a rapid change in temperature, chlorophyll, and salinity distribution, while the horizontal gradients of these properties are homogeneous in the surrounding water masses. Fronts have significant effect on biology. These systems tend to form zones of convergence of different water masses resulting in accumulation of planktonic organisms. This aggregation also affects distribution of secondary producers and pelagic herbivores (Laevastu & Hayes, 1981).

In remote sensing images, the fronts represent boundary between two water masses of different properties. The fronts can be easily delineated in SST and in the ocean color images due to variation in SST and chlorophyll concentrations (Figs. 6, 7). The various types of shape of fronts are significant to fishery resources (Solanki et al., 2001a). For example, the meandering types of fronts occupy larger areas than linear fronts. Fronts with high SST or chlorophyll gradients act as boundary for resources distributions. Fish populations aggregate in frontal boundaries due to accumulation of planktonic organisms. Relevance of oceanic front with fishery resources has been documented by Laurs et al. (1984), Maul et al. (1984) and Solanki et al. (2001a, 2003a, b). The details of statistical analysis of fish catch data and species distribution with reference to habitat have been discussed by Solanki et al. (2005).

Conclusion

Oceanographic spatio-temporal processes are important to fishery resources accumulation. Such processes were identified on satellite images of ocean color and SST derived from IRS-OCM and NOAA, respectively. Important upwelling areas with low SST/high chlorophyll were identified and monitored from formation to stable phases. Fish catch was found to decline during initiation phase, while it increased during maturation and stabilization phases. Cyclonic eddies yielded high biological production leading to high catch inside the eddy areas, while anti-cyclonic eddies were found with low chlorophyll concentration. The frontal structures were identified with high chlorophyll concentrations indicating high biological production and high fish catch. Such satellite observations are useful to monitor ecological associations.

Acknowledgments The authors are grateful to Dr. R. R. Navalgund, Director, Space Applications Centre (SAC), and Dr. K. L. Majumdar, Deputy Director, Remote Sensing and Image Processing Area (RESIPA, SAC) for their interest and encouragement during the execution of this work.

References

Anonymous, 1996. Fish catch Statistics Report for Year 1995. The Commissioner of Fisheries, Fisheries Department, State Government, Gujarat State, Gandhinagar.

Banse, K., 1968. Hydrography of the Arabian Sea Shelf of India and Pakistan, and effect on demersal fisheries. Deep Sea Research 15: 45–79.

Chauhan, P., M. Mohan, P. Matondkar, B. Kumari & S. Nayak, 2002. Surface chlorophyll-a estimation using IRS-P4 OCM data in the Arabian Sea. International Journal of Remote Sensing 23: 1663–1676.

Fiedler, P. C., G. B. Smith & R. M. Laurs, 1985. Fisheries application of satellite data in the eastern North Pacific. Marine Fisheries Review 46: 1–13.

Gordon, H. R., R. W. Austin, D. A. Clark, W. A. Hovis & C. S. Yentsch, 1985. Ocean color measurements. Advances in Geophysics 27: 297–333.

Laevastu, T. & T. Hayes, 1981. Fisheries oceanography. Fishing News Books, Norwich, England: 199.

Laurs, R. M. & J. T. Burcks, 1985. Living marine resources applications. Advances in Geophysics 27: 419–452.

Laurs, R. M., P. C. Fiedler & M. Montegomery, 1984. Albacore catch distributions relative to environmental features observed from satellite. Deep Sea Research 31: 1085–1099.

Maul, G. A., M. Roffer & F. M. Sousa, 1984. Remotely sensed oceanographic patterns and variability of blue fin tuna catch in the Gulf of Mexico. Oceanologica Acta 7: 469–479.

McClain, P. C., W. G. Pichel & C. C. Walton, 1985. Comparative performance of AVHRR based multi channel sea surface temperature. Journal of Geophysical Research 90: 11587–11601.

Mohan, M., P. Chauhan, A. Mathur & R. M. Dwivedi, 1998. Atmospheric correction of MOS-B data using long wavelength and PCI based approaches. Scientific Report, SAC/RESA/MWRD/IRSP3/SN/02/98: 14–22.

Narayana, A., H. U. Solanki, B. G. Krishna & A. Narain, 1995. Geometric correction and radiometric normalisation of NOAA AVHRR data for fisheries application. International Journal of Remote Sensing 16: 765–771.

Njoku, E. G., T. P. Barnett, R. M. Laurs & A. C. Vasano, 1986. Advances in satellite sea surface temperature measurement and oceanographic applications. Journal of Geophysical Research 90: 11571–11586.

O'Reilly, J. E., S. Maritonena, B. G. Mitchell, D. A. Siegal, K. L. Carder, S. A. Graver, M. Kahru & C. R. McClain, 1998. Ocean color chlorophyll algorithms for SeaWiFS. Journal of Geophysics 103: 24937–24963.

Podestra, G. P., J. A. Browder & J. J. Hoey, 1993. Exploring the association between swordfish catch rates and thermal fronts on US longline grounds in the Western North Atlantic. Continental Shelf Research 13: 253–277.

Solanki, H. U., R. M. Dwivedi & A. Narain, 1998a. Satellite observations of coastal upwelling in the Northern Arabian Sea and its impact on fishery resources. Proceedings of the International Symposium on Information Technology in Oceanography (ITO, 1998), October 1998, Goa, India: 12–16.

Solanki, H. U., R. M. Dwivedi & S. R. Nayak, 1998b. Relationship between IRS MOS-B derived chlorophyll and NOAA AVHRR SST: a case study in the North West Arabian Sea, India. Proceedings of 2nd International workshop on MOS-IRS and Ocean Colour. Institute of Space Sensor Technology, Berlin, Germany: 327–339.

Solanki H. U., R. M. Dwivedi & S. R. Nayak, 2000. Generation of composite image using OCM chlorophyll and NOAA AVHRR SST for locating potential fishing grounds. In Proceedings PORSEC 2000 vol II, 669–672.

Solanki H. U., R. M. Dwivedi & S. R. Nayak, 2001a. Synergistic analysis of Sea WiFS chlorophyll and NOAA AVHRR derived SST features for marine living resources. International Journal of Remote Sensing 22(8): 3877–3882.

Solanki H. U., R. M. Dwivedi & S. R. Nayak, 2001b. Application of OCM chlorophyll and AVHRR SST for fishery forecast: Preliminary results off Gujarat coast. Indian Journal of Marine Science 30(3): 132–138.

Solanki, H. U., R. M. Dwivedi & S. R. Nayak, 2003a. Application of remotely sensed closely coupled biological and physical process for marine fishery resources exploration. Journal of Society of Indian Remote Sensing 31: 67–70.

Solanki, H. U., R. M. Dwivedi, S. R. Nayak, V. S. Somvanshi, D. K. Gulati & S. K. Pattnayak, 2003b. Fishery forecast using OCM chlorophyll concentration and AVHRR SST: Validation results of Gujarat Coast, India. International Journal of Remote Sensing 24: 3691–3699.

Solanki, H. U., P. C. Mankodi, S. R. Nayak & V. S. Somvanshi, 2005. Evaluation of remote-sensing-based potential fishing zones (PFZs) forecast methodology. Continental Shelf Research 25: 2163–2173.

Solanki, H. U., M. Raman, B. Kumari, R. M. Dwivedi & A. Narain, 1998c. Seasonal trends in the fishery resources off Gujarat: salient observations using NOAA-AVHRR. Indian Journal of Maine Sciences 27: 438–442.

Stretta, J. M., 1991. Forecasting models for tuna fishery with Aerospatiale remote sensing. International Journal of Remote Sensing 12: 771–779.

Sugimoto, T. & H. Tameish, 1992. Warm core rings and their role on the fishing ground formation around Japan. Deep Sea Research 39: 183–201.

Yamanaka, I., S. Ito, K. Niwa, R. Tanabe, Y. Yabuta & S. Chikuni, 1998. The fisheries forecasting system in Japan for coastal pelagic fish. FAO Fisheries Technical Paper 301: 372.